Biohemistry

pubs.acs.org/biochemistry Article

Novel Noncompetitive Type Three Secretion System ATPase Inhibitors Shut Down *Shigella* Effector Secretion

Heather B. Case, Dominic S. Mattock, Bill R. Miller III, and Nicholas E. Dickenson*



Cite This: Biochemistry 2020, 59, 2667-2678



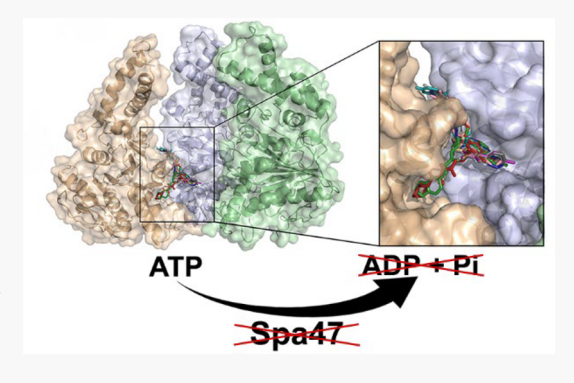
ACCESS

Metrics & More

Article Recommendations

s Supporting Information

ABSTRACT: Shigella is the causative agent of bacillary dysentery and is responsible for an estimated 165 million infections and 600,000 deaths annually. Like many Gram-negative pathogens, Shigella relies on a type three secretion system (T3SS) to initiate and sustain infection by directly injecting effector proteins into host cells. Protein secretion through the needle-like injectisome and overall Shigella virulence rely on the T3SS ATPase Spa47, making it a likely means for T3SS regulation and an attractive target for therapeutic small molecule inhibitors. Here, we utilize a recently solved 2.15 Å crystal structure of Spa47 to computationally screen 7.6 million drug-like compounds for candidates which avoid the highly conserved active site by targeting a distal, but critical, interface between adjacent protomers of the Spa47 homohexamer. Ten of the top inhibitor candidates were characterized, identifying novel Spa47 inhibitors that reduce in vitro ATPase activity by as



much as $87.9 \pm 10.5\%$ with IC₅₀'s as low as $25 \pm 20~\mu\text{M}$ and reduce *in vivo Shigella* T3SS protein secretion by as much as $94.7 \pm 3.0\%$. Kinetic analyses show that the inhibitors operate through a noncompetitive mechanism that likely supports the inhibitors' low cytotoxicity, as they avoid off-target ATPases involved in either *Shigella* or mammalian cell metabolism. Interestingly, the inhibitors display nearly identical inhibition profiles for Spa47 and the T3SS ATPases EscN from *E. coli* and FliI from *Salmonella*. Together, the results of this study provide much-needed insight into T3SS ATPase inhibition mechanisms and a strong platform for developing broadly effective cross-pathogen T3SS ATPase inhibitors.

he first nonflagellar type three secretion systems (T3SS) were identified over 30 years ago in Salmonella¹ and Yersinia.² Since then, T3SSs have been identified as essential virulence factors in many Gram-negative bacterial pathogens including Chlamydia, Burkholderia, Pseudomonas, pathogenic E. coli, and Shigella.³⁻⁵ Each of these pathogens rely on their specialized T3SS(s) to inject bacterial effector proteins directly into the cytoplasm of eukaryotic host cells. 4,6 While the injected T3SS effector proteins are tailored to specifically support the infection mechanisms and replicative niches of the bacteria that express them,⁷ the type three secretion apparatus (T3SA), or injectisome, that supports effector secretion is highly structurally and functionally conserved across the diverse genera of bacteria that rely upon them.^{8,9} The apparatus itself resembles a syringe and needle-like nanomachine that spans the inner and outer bacterial membranes, extends past the associated lipopolysaccharide (LPS) layer, and penetrates the membrane of infected host cells, providing a unidirectional conduit through which the T3SS effector proteins are actively secreted into the host cell cytoplasm to support infection and evasion of host immune responses. 10,11 Structurally, the injectisome is comprised of four main regions: the cytoplasmic region found at the cytoplasmic face of the bacterial inner membrane, a basal body that spans the bacterial inner and outer membranes, a hollow needle-like structure that

extends past the LPS layer, and a hetero-oligomeric protein tip assembly that serves as both an environmental sensor and a transmembrane complex that penetrates the host cell cytoplasmic membrane. ^{12,13}

Despite the clear correlation between T3SS expression/activity and pathogen virulence, the specific mechanisms that support and regulate protein secretion through the apparatus remain largely unclear and are of significant interest for both uncovering bacterial virulence regulation mechanisms and identifying targets for anti-infective therapeutics effective against a broad class of human pathogens. What is understood, however, is that most, if not all, T3SS injectisomes include a highly conserved ATPase at their base whose activity is critical for proper protein secretion through the apparatus and pathogen virulence. 14–17 Furthermore, pioneering studies in Salmonella enterica suggest that these ATPases may specifically be responsible for recognition, chaperone release, and partial

Received: May 22, 2020 **Revised:** June 18, 2020 **Published:** June 22, 2020





unfolding of protein substrates prior to secretion through the injectisome. These findings, together with the recent identification of T3SS proteins and synthetic small molecules capable of inhibiting T3SS ATPase activity, implicate T3SS ATPases as likely means for both native and therapeutic control of T3SS activity and pathogen virulence.

Here, we utilize a series of recently solved high-resolution crystal structures of the *Shigella* T3SS ATPase, Spa47, to computationally screen 7.6 million drug-like compounds and identify novel, highly specific, noncompetitive T3SS ATPase inhibitors that effectively prevent *in vitro* ATPase activity of Spa47 and *in vivo* T3SS function within *S. flexneri*. Additionally, the identified Spa47 inhibitors were evaluated against homologous T3SS ATPases from enteropathogenic *E. coli* and *Salmonella enterica*. Insights into the relationship between T3SS activity and T3SS function as well as trends in inhibition profiles among T3SS ATPase isozymes are discussed, providing valuable insight into Spa47 regulation of protein secretion and laying the groundwork for the development of cross-pathogen T3SS ATPase inhibitors.

■ EXPERIMENTAL PROCEDURES

Materials. Wild-type Shigella flexneri corresponds to the serotype 2a 2457T strain originally isolated in 1954.²⁶ The S. flexneri spa47 null strain was engineered by Abdelmounaaim Allaoui as described by Jouihri et al. 15 The Superdex 200 Increase 16/600 and Superdex 200 Increase 5/150 size exclusion columns, and 5 mL of HiTrap Q FF columns were purchased from GE Healthcare (Pittsburgh, PA). Chitin resin was from New England Biolabs (Ipswich, MA). ATP and Congo red were from Sigma-Aldrich (St. Louis, MO). Dithiothreitol (DTT) and ampicillin were from Gold Biotechnology (St. Louis, MO). The malachite green assay kit was purchased from BioAssay Systems (Hayward, CA). Rabbit polyclonal antibodies against IpaC were a generous gift from Wendy and William Picking (University of Kansas). The conjugated monoclonal anti-GAPDH antibody was from Thermo Scientific (Waltham, MA), and the Alexa 647 goat anti-rabbit secondary antibody was from Life Technologies (Carlsbad, CA). The Spa47 inhibitors 8573, 3812, 8771, 4000, and 1870 were from Enamine (Monmouth Jct., NJ), 4967 was from ChemBridge (San Diego, CA), and inhibitors 2357, 6573, 5765, and 1691 were from ChemDiv (San Diego, CA). All other solutions and chemicals were of reagent grade. The UniProtKB accession numbers for Spa47, F1 ATP synthase (α subunit), F1 ATP synthase (β -subunit), EscN, FliI, InvC, SsaN, YscN, and CdsN are P0A1C1, P25705, P06576, Q9AJ15, P26465, B5RDL8, P74857, P40290, and F8KX49 respectively.

In Silico Small Molecule Spa47 Inhibitor Screen. An oligomeric Spa47 model was generated for computational small molecule docking analysis by aligning a 2.15 Å monomeric Spa47 structure (PDB entry 5SYP)²⁷ to each protomer of the 2.8 Å heterohexameric F1 $\alpha_3\beta_3$ ATP synthase structure (PDB code 1BMF)²⁸ using PyMol,²⁹ as described previously.²⁷ The resulting hexamer structure was energy minimized using Discover Studio ViewerPro.³⁰ Two aligned Spa47 monomers were extracted to provide a representative dimeric interface with a complete ATPase active site for subsequent docking analyses.

A selection of small molecules for testing was obtained from the Zinc Database³¹ by selecting all 3D in stock, reference pH, structures with molecular weights of 250 to 500 Da, and logP

values from -1 to 4. These filters resulted in a selection of 7.6 million compounds which were prepared for docking analyses as .pdbqt files using Open Babel. 32 Potential interactions were limited to a 30 Å³ docking region (centered at x,y,z =121,101,76) that included a portion of the Spa47 protomer interface that we have shown previously to play critical roles in oligomerization and Spa47 activation.³³ Docking of compounds to the Spa47 interface was then conducted using QuickVina2,³⁴ predicting both binding location and affinities. During docking, the protein structure and amino acids side chains were held static, while the searching algorithm generated different conformations of the ligands around their rotatable bonds using the default exhaustiveness settings in QuickVina2. Ten small molecule inhibitor candidates were chosen for experimental validation based upon predicted binding location, calculated binding affinity, and solubility. The selected compounds and their characteristics are included in Table S1.

Protein Expression and Purification. The spa47 gene was cloned into the plasmid pWPsf4 for expression in Shigella and pTYB21 for expression in E. coli, as described previously.³⁵ The genes encoding EscN and FliI were additionally cloned into pTYB21 using the SapI and PstI restriction sites. Spa47, EscN, and FliI encoded in pTYB21 were independently transformed into E. coli Tuner (DE3) cells and expressed and purified as previously described for Spa47.35 Briefly, the E. coli Tuner (DE3) expression strain was grown to an OD₆₀₀ \sim 0.8 in Terrific Broth (TB) medium containing 0.1 mg/mL ampicillin at 37 °C and 200 rpm. The culture was then cooled to 17 °C before induction with 1 mM isopropyl β -D-1-thiogalactopyranoside (IPTG) for ~20 h (17 °C, 200 rpm). All subsequent steps were carried out at 4 °C unless otherwise stated. The cells were pelleted by centrifugation, resuspended in binding buffer (20 mM Tris, 500 mM NaCl, 48 mg/L 4-(2aminoethyl) benzenesulfonyl fluoride hydrochloride (AEBSF), pH 7.9), and lysed by sonication. The sonicated product was then centrifuged, and the supernatant was run over a chitin affinity column to capture the chitin binding domain (CBD)-intein-ATPase fusion complex. The purified proteins (Spa47, EscN, and FliI) were eluted from the column by intein cleavage in binding buffer containing 50 mM DTT. The elution fractions were pooled and diluted using 20 mM Tris buffer to reduce the final NaCl concentration to 100 mM and the final DTT concentration to 10 mM. The proteins were further purified by negative selection over a 5-ml Q Sepharose FF anion exchange column. The purified protein in the anion exchange flow-through was concentrated using an ultracentrifugal filter unit with a 30-kDa molecular mass cutoff and further purified/characterized using a Superdex 200 16/ 600 size exclusion column equilibrated with 20 mM Tris, 100 mM NaCl, 5 mM DTT, pH 7.9. Protein concentrations were determined using in-gel densitometry of Coomassie-stained protein with bovine serum albumin (BSA) as a standard (as previously validated).³⁵ All Spa47, EscN, and FliI concentrations are reported in monomer concentration units for consistency and clarity.

Kinetic Analysis of Spa47. Spa47 ATPase activity was measured using a malachite green phosphate quantitation kit according to manufacturer guidelines. The putative small molecule inhibitors were dissolved in DMSO to a concentration of 20 mM, and the final concentration of DMSO in each ATPase reaction was maintained at 2.5%. We have previously shown that DMSO concentrations as high as 12.5%

do not negatively impact Spa47 oligomer ATPase activity; however, only 2.5% DMSO was required to maintain solubility of the inhibitors tested in this study. The effect of the inhibitors on the rate of ATP hydrolysis was examined on SEC-isolated oligomeric Spa47 at 22 °C in 20 mM Tris (pH 7.9), 100 mM NaCl, 5 mM DTT, 10 mM MgCl₂, and 2.5% DMSO. For the initial inhibition screening, ATPase activity was quantified for 0.05 μ M Spa47 in the absence and presence of each of the ten tested inhibitors (250 μ M). Inhibitors that resulted in \geq 50% inhibition at 250 μ M were then evaluated by full kinetic inhibition analysis and effect on *Shigella* T3SS function.

Inhibitor IC₅₀ values were determined for the most potent inhibitors by holding the concentration of Spa47 constant at 0.05 μ M and quantifying ATPase activity in the presence of increasing concentrations of the inhibitors (0 μ M, 25 μ M, 50 μ M, 100 μ M, 250 μ M, and 500 μ M). IC₅₀'s were calculated by fitting the resulting data to a four-parameter logistic sigmoidal dose response curve resulting from triplicate analyses.

Substrate-dependent kinetic analyses were performed on Spa47 in the presence of varying inhibitor and substrate (ATP) concentrations. The Spa47 and DMSO concentrations were held constant at 0.05 μ M and 2.5%, respectively, while the inhibitor concentrations tested included 0 μ M, 50 μ M, 225 μ M, and 500 μ M. Initial ATP hydrolysis velocities were determined at each inhibitor concentrations in the presence of 0.025 mM, 0.075 mM, 0.150 mM, 0.300 mM, and 0.600 mM ATP. The initial velocities were plotted as a function of substrate (ATP) concentration, and SigmaPlot 12 was used to fit each data set to the Michaelis–Menten equation (eq 1):

$$\nu = \frac{V_{\text{max}}[S]}{K_{\text{M}} + [S]} \tag{1}$$

where ν is the initial velocity of the reaction, [S] is the ATP concentration, $K_{\rm M}$ is the Michaelis constant, and $V_{\rm max}$ is the maximum velocity of the enzyme. The inhibition profiles were additionally fit and modeled using VisualEnzymics to determine the mode of inhibition for each of the tested inhibitors.

In addition to evaluating the effect of the predicted inhibitors on Spa47, each inhibitor was evaluated for effect on the ATPase activity of EscN and FliI. As done for Spa47, all conditions were tested in the presence of 20 mM Tris (pH 7.9), 100 mM NaCl, 5 mM DTT, 10 mM MgCl₂, and 2.5% DMSO. Due to differences in basal activity levels and temperature dependency, EscN was tested at a final enzyme concentration of 0.05 μ M (22 °C), and FliI was evaluated at a final concentration of 0.5 μ M at 32 °C. All tests were performed in triplicate in the presence and absence of 250 μ M inhibitor.

Effect of Spa47 Inhibitors on Shigella Growth Profiles. An S. flexneri strain expressing wild-type Spa47 was grown overnight on a tryptic soy agar (TSA)-Congo red plate, and a small number of isolated colonies were used to inoculate 10 mL of tryptic soy broth (TSB). The inoculated culture was grown to OD₆₀₀ 0.05, and a small amount was diluted and plated onto a TSA-Congo red plate as time point zero for the collected growth curves. The parent culture was then split into 1 mL subcultures containing 2.5% DMSO and 500 μ M inhibitor, as we have previously shown that concentrations as high as 5% DMSO have a negligible effect on Shigella culture growth profiles. ²⁰ In addition to the tested inhibitor

conditions, a control flask containing no inhibitor, but 2.5% DMSO was included for comparison. Several of the inhibitors absorb across the visible spectrum and interfere with optical density readings of the cultures, so a small culture sample was taken from each flask, diluted, and spread on TSA-Congo red plates every hour for 8 h to quantify culture growth/density. The plates were incubated overnight at 37 °C, and the colonies were counted to generate growth curves for the control culture and the cultures containing each inhibitor.

Effect of Spa47 Inhibitors on HeLa Cell Viability. An MTT colorimetric assay was used to quantify the cytotoxic effects of the small molecule T3SS ATPase inhibitors on HeLa cells. HeLa cells purchased from the American Type Culture Collection (ATCC) were passaged according to ATCC protocol and seeded in a sterile 96-well plate. The cells were incubated overnight in DMEM supplemented with 10% fetal calf serum and a penicillin/streptomycin antibiotic cocktail at 37 °C, 100% humidity, and 5% CO_2 . The cells were then incubated under identical environmental conditions (37 °C, 100% humidity, and 5% CO_2) for 30 min with 100 μ M inhibitor and 1% DMSO prior to the addition of MTT. The cells were then incubated for an additional 4 h with 100 μ M inhibitor, 1% DMSO, and MTT at 37 °C prior to the addition of 200 μ L of DMSO to fully dissolve the produced formazan salt. The formazan levels produced by viable cells in each well were then compared to control conditions where the cells were not exposed to the inhibitors by measuring the absorbance of each condition at 570 nm.

Quantitation of S. flexneri T3SS Translocator Secretion. The small diazo dye Congo red effectively induces active secretion of translocator proteins through the Shigella T3SS by mimicking the natural trigger resulting from host cell membrane interaction.³⁶ Thus, Congo red exposure serves as a valuable tool that allows for rapid activation of Shigella type three secretion. Briefly, a S. flexneri strain lacking the gene for Spa47 and a strain expressing wild-type Spa47 were grown overnight on TSA-Congo red plates, and a small number of isolated colonies were used to inoculate 15 mL of TSB containing appropriate antibiotics. Cultures were grown at 37 °C to OD₆₀₀ 0.05, and the wild-type Shigella strain was split into 1 mL subcultures with 500 μ M inhibitor and 2.5% DMSO. Control growths (1 mL) of Shigella lacking Spa47 and Shigella expressing wild-type Spa47 (2.5% DMSO, but no inhibitor) were also prepared. All cultures were grown to an OD₆₀₀ of ~1.0. The cultures were centrifuged at 2272g and rinsed to separate the bacteria from the culture supernatant and any proteins that had been secreted up to that point. The cells were then resuspended in sodium phosphate buffer containing 0.28 mg/mL Congo red, the appropriate inhibitor, 2.5% DMSO, and were incubated at 37 °C for 30 min to promote active type three secretion. Cultures were then chilled on ice for 5 min to limit further secretion, and the bacteria were separated from the protein-containing supernatant by centrifugation at 13 000g for 15 min at 4 °C. The secreted proteins within the supernatant from each condition were separated using SDS-PAGE, transferred to polyvinylidene difluoride (PVDF) membranes by Western blot, and probed using anti-IpaC rabbit polyclonal antibodies and Alexa 647 goat anti-rabbit secondary antibodies. Secreted IpaC levels were compared using a Bio-Rad ChemiDoc imaging system and the associated Image Lab analysis software. As validated previously, 37,38 a monoclonal antibody against the cytoplasmic enzyme glyceraldehyde-3-phosphate dehydrogenase (GAPDH) was used as a

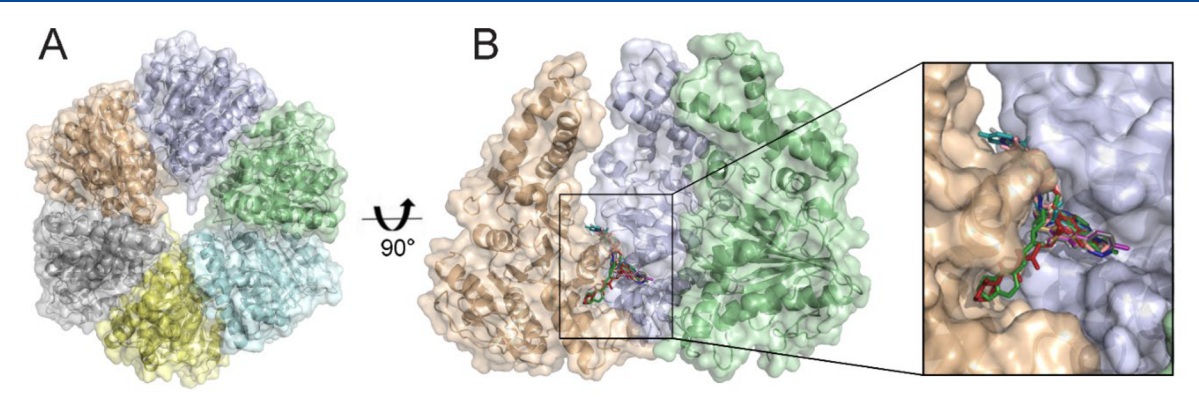


Figure 1. Docking calculations identify Spa47 inhibitor candidates. (A) Top view of the activated homohexameric Spa47 model with each promoter colored independently. (B) The model is rotated up 90° with the front three protomers removed to clearly display the predicted binding locations of the ten inhibitor candidates tested in this study. A zoomed in view of the promoter interface illustrates the locations where the inhibitors are predicted to bind.

nonsecreted control protein in the Western blot to ensure that IpaC detected in the supernatant is the result of protein secretion and not cell lysis. The anti-IpaC antibodies have been used in effector secretion assays previously^{27,33,38} and have been validated against both purified IpaC protein and *Shigella* whole cell lysates in which they specifically recognize IpaC in a wild-type *Shigella* strain, but not in a strain lacking the gene for IpaC.

Effect of Spa47 ATPase Inhibitors on Spa47 Oligomer State. Because we targeted the inhibitors to the interface of Spa47 protomers in the active oligomer, we tested the ability of each of the inhibitors to disrupt Spa47 oligomers, an event that would effectively inhibit ATPase activity. Size exclusion chromatography (SEC) was performed on isolated Spa47 oligomers in both the absence and presence of each of the small molecule inhibitors. Specifically, Spa47 was purified as described above and the active oligomer was isolated via SEC. At room temperature, 22 μ M Spa47 was then incubated in 500 μM inhibitor and 2.5% DMSO for 30 min before it was analyzed using a Superdex 200 increase 5/150 size exclusion column equilibrated with 20 mM Tris (pH 7.9), 100 mM NaCl, 5 mM DTT, and 2.5% DMSO and run at 0.1 mL/min. Control conditions included isolated monomeric and oligomeric Spa47 in the absence of inhibitors, but in the presence of 2.5% DMSO, which was previously determined not to affect the distribution of Spa47 oligomers.

RESULTS

High-throughput In Silico Screening of Potential Shigella T3SS ATPase Inhibitors. Spa47 ATPase activation requires homo-oligomerization to complete the interfacial active sites within the activated complex predicted to reside at the base of the T3SA as a homohexamer. 12,27,38 A recently solved 2.15 Å Spa47 crystal structure of Spa47²⁷ was modeled onto the hexameric structure of F1 ATP synthase²⁸ and energy minimized using Discover Studio ViewerPro. 30 Two adjacent Spa47 protomers were extracted from the model and were used for an *in silico* screen of 7.6 million drug like compounds from the ZINC Database,³¹ specifically screening for compounds that bind at the protomer interface while avoiding the highly conserved enzyme active site. Of the 7.6 million screened small molecules, the top 1000 (based on calculated binding energy) were manually examined and narrowed down based on predicted binding affinity, solubility (logP), predicted binding location, and commercial availability. Inhibitors

predicted to strongly bind within or in close proximity to the active site were eliminated to increase the chances of identifying noncompetitive Spa47 inhibitors and minimize off-target inhibition of non-T3SS ATPases. Interestingly, many of the inhibitor binding interactions predicted by the screen localized to a single region of the interface between the Spa47 protomers, despite significant differences in chemical characteristics between many of the putative inhibitors (Figure 1 and Table S1). The ten inhibitors displayed in Figure 1 and Table S1 were then purchased and tested for both *in vitro* inhibition of ATPase activity and *in vivo* inhibition of T3SS function.

Predicted Small Molecule T3SS Inhibitors Are Effective against the Shigella T3SS ATPase Spa47. The ten compounds selected from the in silico screen (8573, 4967, 3812, 6573, 8771, 2357, 1691, 5765, 4000, and 1870) were tested for their effect on Spa47 ATPase activity using a colorimetric malachite green activity assay. The ATPase activity of activated oligomeric Spa47 was tested at 0.05 μ M in the absence and presence of 250 μ M of each putative inhibitor (Figure 2). The effectiveness of the tested inhibitors ranged from 1.5 \pm 16.0% to 87.9 \pm 10.5% inhibition, with

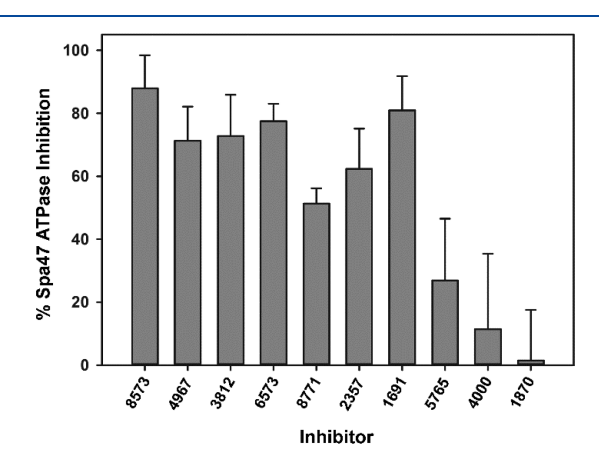


Figure 2. Novel Spa47 inhibitors efficiently reduce ATPase activity *in vitro*. The ATPase activity of isolated oligomeric Spa47 was tested in the presence of each of the 10 small molecules selected from the *in silico* screen. Spa47 and inhibitor concentrations were 0.05 μ M and 250 μ M, respectively. Percent inhibition was calculated by comparing ATPase activity for each inhibitor condition to Spa47 activity in the absence of inhibitor. Data are plotted as the mean \pm SD from three independent analyses.

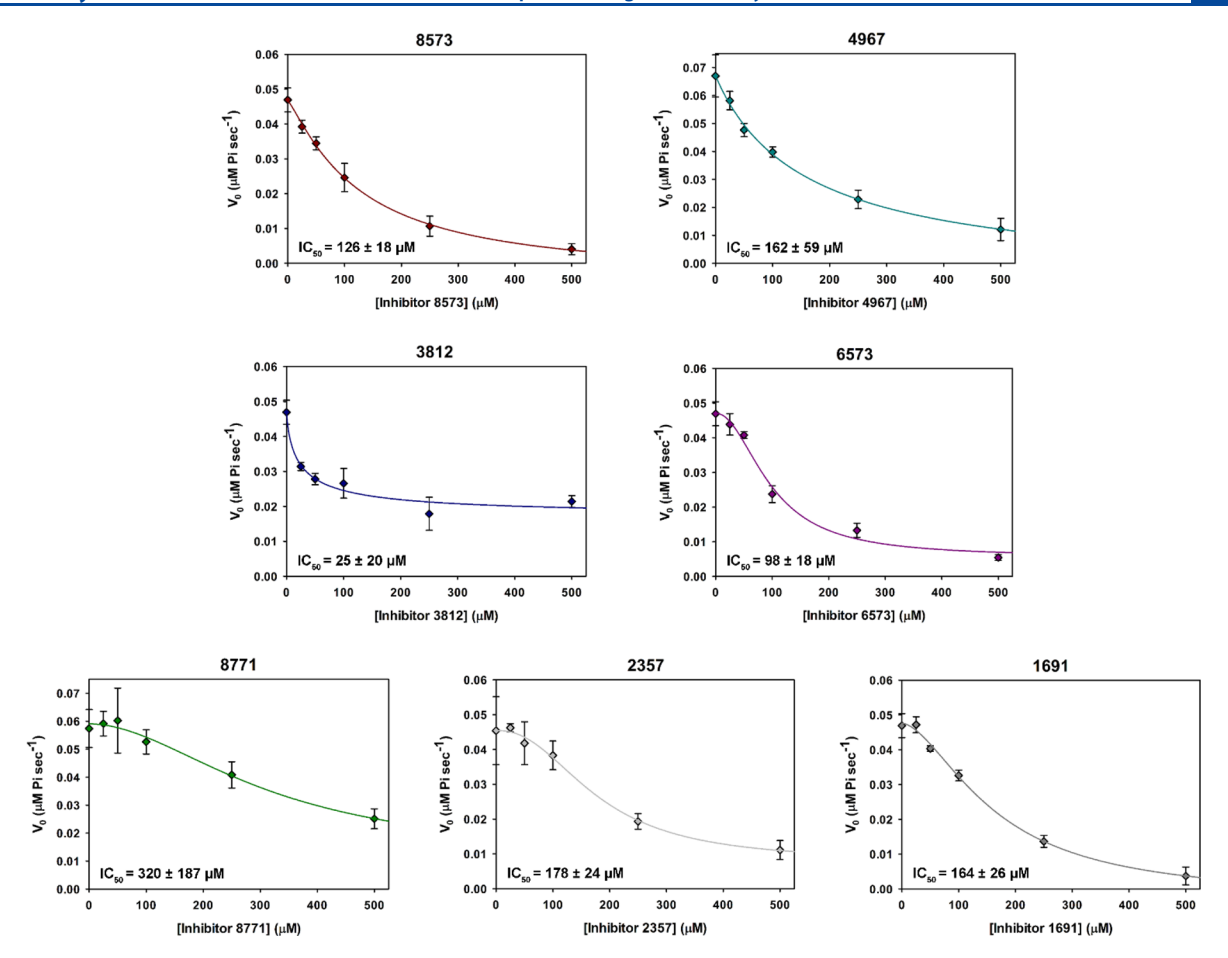


Figure 3. Concentration-dependence of Spa47 inhibition. Spa47 ATPase activity was measured in the presence of increasing concentrations of inhibitor. The resulting inhibition profiles for each compound were fit to a four parameter logistic sigmoidal dose response curve to determine IC_{50} values. Data are plotted as the mean \pm SD from three independent analyses.

seven of the ten inhibitors resulting in a greater than 50% reduction in Spa47 activity and five of the ten inhibitors providing greater than 70% inhibition. The three candidates that provided less than 50% inhibition of Spa47 (inhibitors 5765, 4000, and 1870) were deemed ineffective and were not included in the subsequent *in vitro* and *in vivo* analyses described below.

 IC_{50} 's were determined for the seven inhibitors that reduced Spa47 activity by greater than 50%. The tested inhibitors were titrated into 0.05 μ M Spa47, and initial reaction velocity was plotted as a function of inhibitor concentration (Figure 3). The data were fit to four-parameter logistic sigmoidal dose response curves, quantifying IC_{50} 's that range from 25 \pm 20 μ M to 320 \pm 187 μ M for inhibitors 3812 and 8771, respectively.

Novel Noncompetitive Shigella T3SS ATPase Inhibitors Avoid Off-Target Metabolic ATPases. Shigella flexneri replicates rapidly both in culture and within the cytoplasm of infected host cells, exhibiting 30 to 40 min doubling times in both environments. Furthermore, with no selective pressure in liquid media, Shigella growth rates are not significantly influenced by the presence or functionality of its T3SS, and as expected for robust Gram-negative bacteria, they are unaffected by DMSO concentrations as high as 5%. To ensure that the tested inhibitors are specific for Spa47 and do not reduce the overall metabolic activity of the bacteria or inhibit "housekeeping" ATPases critical for bacterial growth and survival, the effect of the inhibitors on Shigella growth

curves was examined. Growth curves were generated for an S. flexneri strain expressing wild-type Spa47 in TSB liquid media cultures containing 2.5% DMSO and in the absence or presence of 500 μ M inhibitor (Figure 4A). The growth curves resulting from exposure to each of the tested inhibitors closely match that of the control culture, indicating that the inhibitors do not adversely affect Shigella metabolism or affect critical off-target Shigella ATPases.

An MTT cytotoxicity assay was performed on cultured HeLa cells to test the effect of the identified Spa47 inhibitors on mammalian cell viability. HeLa cell membranes are much less robust than the cell wall of *Shigella*, limiting the DMSO concentration to 1% which, due to solubility, reduced the maximum inhibitor concentrations to 100 μ M. Figure 4B shows percent HeLa cell toxicity following a 4.5 h exposure to each tested inhibitor. Notably, inhibitors 8573, 6573, 8771, 2357, and 1691 resulted in limited cytotoxic effects with values of 0.9 \pm 2.7%, 0.8 \pm 8.5%, 7.9 \pm 3.1%, 3.5 \pm 11.8%, and 1.6 \pm 11.0% cytotoxicity, respectively. Inhibitors 4967 and 3812 were 33.1 \pm 7.2% and 18.6 \pm 8.8% cytotoxic, respectively.

Spa47 Inhibitors Prevent Secretion of the Shigella T3SS Effector Protein IpaC. The small diazo dye Congo red can be used to induce secretion of effector proteins through the Shigella T3SS.³⁶ Here, we took advantage of this property and used the well-characterized Congo red-induction secretion assay to measure the effect the identified Spa47 inhibitors had on Shigella type three secretion levels in vivo. Shigella cultures

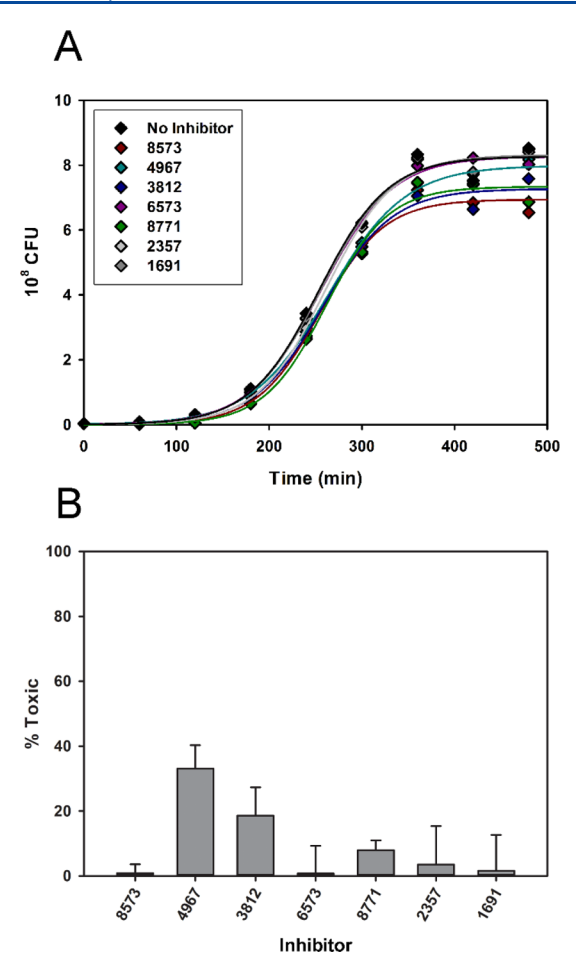


Figure 4. Spa47 ATPase inhibitors avoid off target ATPases. (A) A *Shigella* strain expressing wild-type Spa47 was grown in the presence and absence of 500 μ M inhibitor. Dilution plating was performed hourly for each condition and colony forming units (CFU) are plotted as a function of time and fit to a 3 parameter sigmoidal function, showing that each inhibitor culture has nearly identical growth rates as the culture grown in the absence of inhibitor. (B) An MTT cytotoxicity assay was performed on HeLa cells in the presence and absence of 100 μ M inhibitor. The percent toxicity was determined for each inhibitor, and the data are plotted as the mean \pm SD from three independent analyses.

were grown in 2.5% DMSO and 500 μ M inhibitor and were exposed to Congo red to mimic native secretion activation. The levels of the secreted *Shigella* translocator protein IpaC were quantified via Western blot analysis (Figure 5). With the exception of inhibitor 1691, each of the tested inhibitors resulted in a significant reduction in IpaC secretion levels. Inhibitors 3812 and 8771 proved to be the most effective inhibitors in vivo, reducing T3SS effector secretion by 76.3 \pm 11.1% and 94.7 \pm 3.0%, respectively. The cytoplasmic protein GAPDH was additionally probed as a control and confirmed to be absent in each secretion sample, but present in the whole cell extract, verifying that the detected/quantified IpaC was the result of protein secretion and not cell lysis.

Spa47 Inhibitors Do Not Disrupt Active Spa47 Oligomers. Spa47 is an oligomerization-dependent ATPase that requires homo-oligomerization to assemble active sites between adjacent protomers within the complex. The reliance of Spa47 activity on oligomerization, together with the predicted interfacial binding sites of the inhibitors, led us to

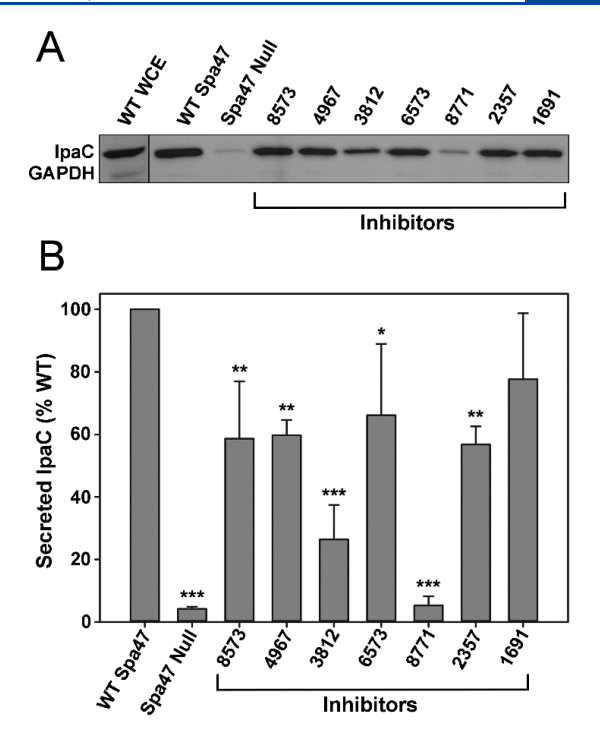


Figure 5. Spa47 Inhibitors prevent secretion of the T3SS effector IpaC. (A) Representative Western blot of secreted IpaC following Congo red activation of *Shigella* cultures treated with 500 μ M of each Spa47 inhibitor and 2.5% DMSO. Control conditions include both a Spa47 null *S. flexneri* strain and an *S. flexneri* strain expressing wild-type Spa47 cultured in 2.5% DMSO but in the absence of inhibitor. The cytoplasmic enzyme GAPDH was observed in the whole cell extracts (WCE) but not in the supernatant containing the secreted IpaC protein. (B) The secreted IpaC levels are reported relative to the *S. flexneri* strain expressing wild-type Spa47 and represent the mean \pm SD from three independent analyses. Significance in IpaC secretion levels between the wild-type Spa47 strain in the absence and presence of the indicated inhibitor is indicated with asterisks (one-way ANOVA followed by a Dunnett's post test. * $p \leq 0.05$, ** $p \leq 0.01$, and *** $p \leq 0.001$).

test whether the inhibitors function through disruption of Spa47 oligomers. Isolated/active Spa47 oligomers were incubated for 30 min in reaction buffer containing 2.5% DMSO and 500 μ M each inhibitor prior to evaluation using a Superdex 200 increase 5/150 size exclusion column. Figure 6 demonstrates that isolated monomeric and oligomeric Spa47 are easily distinguishable based on their elution volumes while the elution profiles of oligomeric Spa47 incubated with any of the seven inhibitors remain unchanged and elute in a single peak at ~1.3 mL, identically to the Spa47 oligomer control.

Kinetic Analyses Elucidate Noncompetitive Inhibition Mechanisms. Full kinetic analyses were performed on the four Spa47 inhibitors that exhibited promising results in the initial *in vitro* and *in vivo* characterizations. To do so, substrate concentration-dependent Spa47 activity profiles were collected at 0 μ M, 50 μ M, 225 μ M, and 500 μ M inhibitor concentrations (Figure 7). Each of the data sets were fit to the Michaelis—Menten equation to calculate the apparent $V_{\rm max}$ and apparent $K_{\rm M}$ values under the same conditions (Table 1). The baseline $V_{\rm max}$ and $K_{\rm M}$ values determined at 0 μ M inhibitor concentration are consistent with our previously published values. The kinetic data collected in the presence of each of the tested inhibitors is consistent with a noncompetitive inhibition mechanism, resulting in a clear decrease in the

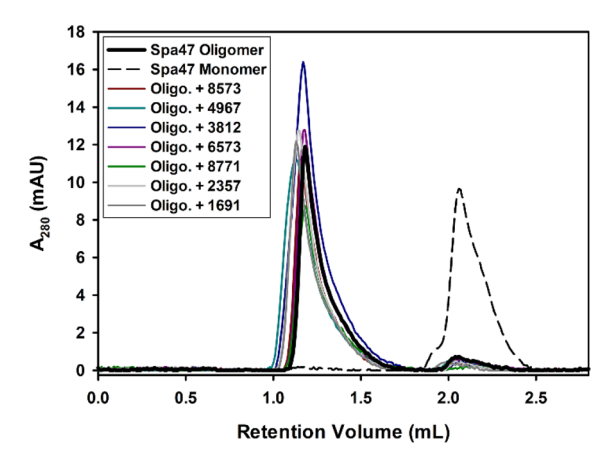


Figure 6. The tested Spa47 ATPase inhibitors do not disrupt Spa47 oligomers. Isolated oligomeric Spa47 was incubated with 500 μ M inhibitors and 2.5% DMSO prior to analysis by size exclusion chromatography. The Spa47 oligomer control and Spa47 oligomer incubated with each inhibitor eluted from the column at \sim 1.3 mL while the Spa47 monomer control eluted at \sim 2.1 mL, consistent with previous analysis showing that the oligomer elutes substantially earlier than the monomer and after the void volume of the column (1.1 mL).

apparent $V_{\rm max}$ and little/no effect on the apparent $K_{\rm M}$. The inhibition kinetics data for each inhibitor were additionally fit to multiple potential inhibition profiles using the software package VisualEnzymics, finding that each inhibitor profile did indeed fit best to a noncompetitive inhibition model. While very few noncompetitive T3SS ATPase inhibitors have been characterized to date, these results are not surprising

considering that the original selection criteria for choosing the putative inhibitors for this study included their predicted interaction at the interface of protomers within the oligomeric Spa47 model and exclusion from the active site.

Shigella T3SS ATPase Inhibitors are Effective against Isozymes from other Pathogens. T3SS ATPases often share significant sequence and structural homology, and it is tempting to speculate that inhibitors designed for one T3SS ATPase may also be effective against T3SS ATPases expressed by related pathogens. Here, we tested the effect of the ten Spa47 inhibitors characterized in this study against the T3SS ATPases EscN from enteropathogenic Escherichia coli (EPEC) and the flagellar T3SS ATPase FliI from Salmonella which share 40.1% and 37.4% sequence identity with Spa47, respectively. In general, the tested inhibitors demonstrate remarkably similar effects on Spa47, EscN, and FliI ATPase activity (Figure 8). The only exceptions to this pattern stem from inhibitors 1691 and 5765, which exhibit similar inhibition effects on Spa47 and EscN but have essentially no effect on FliI ATPase activity. While we hypothesized that there would be some correlation between the effects from the identified Spa47 inhibitors on the tested T3SS ATPase isozymes, the strength of the correlation seen here supports the potential for crosspathogen T3SS ATPase inhibitors as tools for both dissecting the role(s) of T3SS ATPases in type three secretion and pathogen virulence and the development of small molecule therapeutics that target T3SS ATPases and provide broad protection against many high-priority human pathogens.

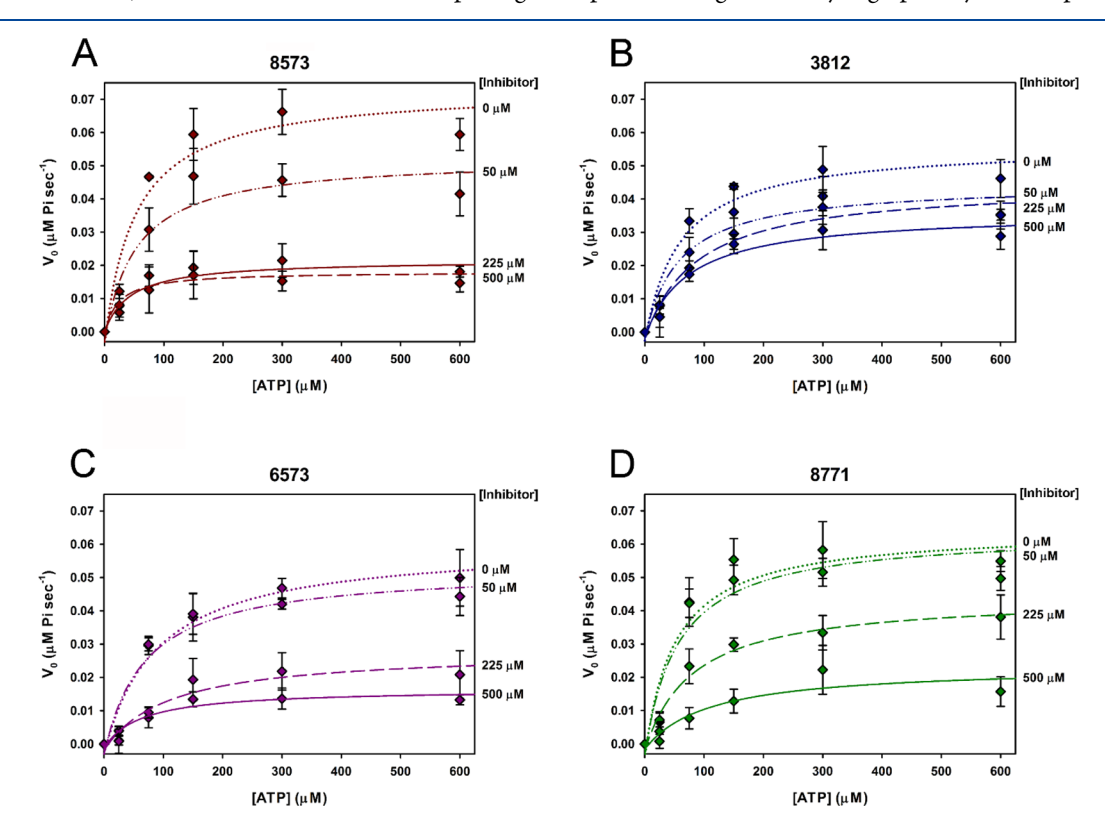


Figure 7. Kinetic inhibition analyses of Spa47. The effect of each inhibitor on Spa47 substrate concentration dependence was tested by plotting initial reaction velocities as a function of ATP concentration. The kinetic analyses were performed in the presence of 0 μ M, 50 μ M, 225 μ M, and 500 μ M. (A) Inhibitor 8573, (B) inhibitor 3812, (C) inhibitor 6573, and (D) inhibitor 8771. Data are plotted as the mean \pm SD from three independent analyses, and **A**–**D** were fit to the Michaelis–Menten equation.

Table 1. Effect of Identified Inhibitors on Substrate-Dependent Spa47 Enzyme Kinetics^a

Inhibitor	Concentration	$K_{\rm M}^{b}~(\mu{\rm M})$	$V_{\rm max}~(\mu{ m M~s^{-1}})$	$k_{\text{cat}}^{c} (s^{-1})$	$k_{\rm cat}/K_{\rm M}~({\rm M}^{-1}~{\rm s}^{-1})$
8573					
	$0~\mu\mathrm{M}$	52 ± 30	0.08 ± 0.01	1.5 ± 0.2	$(3.0 \pm 1.8) \times 10^4$
	50 μM	52 ± 37	0.06 ± 0.01	1.1 ± 0.2	$(2.1 \pm 1.5) \times 10^4$
	$225~\mu\mathrm{M}$	23 ± 24	0.02 ± 0.01	0.4 ± 0.1	$(1.6 \pm 1.7) \times 10^4$
	500 μM	44 ± 20	0.02 ± 0.00	0.4 ± 0.1	$(1.0 \pm 0.5) \times 10^4$
3812					
	$0~\mu\mathrm{M}$	59 ± 31	0.06 ± 0.01	1.2 ± 0.2	$(2.0 \pm 1.1) \times 10^4$
	50 μM	58 ± 33	0.05 ± 0.01	0.9 ± 0.1	$(1.6 \pm 0.9) \times 10^4$
	225 μM	88 ± 41	0.05 ± 0.01	0.9 ± 0.1	$(1.1 \pm 0.5) \times 10^4$
	500 μM	73 ± 36	0.04 ± 0.01	0.8 ± 0.1	$(1.0 \pm 0.5) \times 10^4$
6573					
	$0~\mu\mathrm{M}$	89 ± 40	0.06 ± 0.01	1.3 ± 0.2	$(1.4 \pm 0.7) \times 10^4$
	50 μM	69 ± 39	0.06 ± 0.01	1.1 ± 0.2	$(1.6 \pm 0.9) \times 10^4$
	225 μΜ	109 ± 79	0.03 ± 0.01	0.6 ± 0.1	$(0.6 \pm 0.4) \times 10^4$
	500 μM	63 ± 46	0.02 ± 0.00	0.4 ± 0.1	$(0.6 \pm 0.4) \times 10^4$
8771					
	$0~\mu\mathrm{M}$	50 ± 40	0.07 ± 0.02	1.4 ± 0.3	$(2.7 \pm 2.2) \times 10^4$
	50 μM	56 ± 34	0.07 ± 0.01	1.3 ± 0.2	$(2.4 \pm 1.5) \times 10^4$
	225 μM	81 ± 36	0.05 ± 0.01	0.9 ± 0.1	$(1.1 \pm 0.5) \times 10^4$
	500 μM	108 ± 107	0.03 ± 0.01	0.5 ± 0.1	$(0.5 \pm 0.5) \times 10^4$
	•			1	` ′

"Initial Spa47 reaction velocities were measured as a function of substrate (ATP) and inhibitor concentration. b Apparent $K_{\rm M}$ and $V_{\rm max}$ values \pm the standard error were determined by fitting the mean values from three independent experiments to the Michaelis—Menten equation. Apparent $k_{\rm cat}$ and $k_{\rm cat}/K_{\rm M}$ values \pm the standard error were calculated using the apparent $K_{\rm M}$ and $V_{\rm max}$ values in the table.

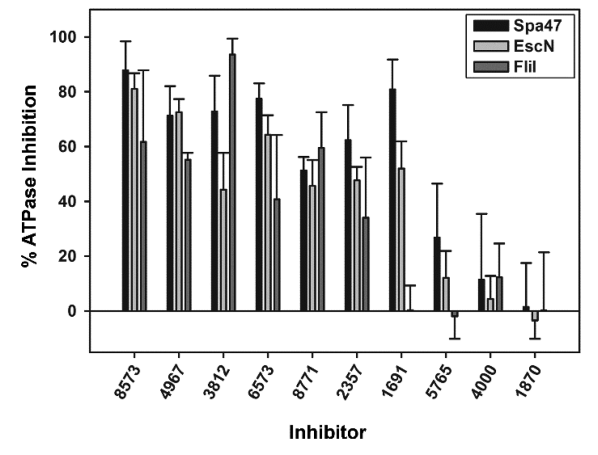


Figure 8. Effect of Spa47 ATPase inhibitors on the isozymes EscN and FliI from *E. coli* and *Salmonella*, respectively. The effect of each Spa47 inhibitor was tested on EscN and FliI ATPase activity. Percent inhibition was determined by incubating 0.05 μ M EscN and 0.5 μ M FliI with 250 μ M inhibitor and comparing ATP hydrolysis to a control condition containing no inhibitor. The Spa47 inhibition data from Figure 2 are included for comparison. Data are plotted as the mean \pm SD from three independent analyses.

DISCUSSION

Type three secretion systems (T3SS) are complex nanomachines that many Gram negative pathogens employ as critical virulence factors. ^{4,6,40} These impressive secretion systems have evolved to simultaneously inject bacterial effector proteins across three membranes (two bacterial and one host) providing direct access to the host cell cytoplasm. Once injected, the effectors subvert host cell functions to support infection and evade immune responses. ^{41–43} Despite the unique, pathogen-specific roles that the diverse effector proteins perform following secretion, the overall architecture and function of the type three secretion system injectisome

remain highly conserved and a likely target for both native and therapeutic regulation of pathogen virulence. Early insight into potential regulatory mechanisms uncovered environmental factors such as temperature, 44,45 NaCl concentrations, 46 bile salts, 47–49 calcium, 50 and specific membrane lipids 51,52 as playing critical roles in controlling pathogen virulence through mechanisms ranging from transcriptional regulation of T3SS genes to maturation of the injectisome tip complex and induction of protein secretion. More recently, studies spanning T3SSs from several pathogens have begun to uncover the functional roles of proteins located within the basal body and cytoplasmic sorting platform of the injectisome, determining that many, if not all, T3SSs require ATPase activity by a homooligomeric AAA ATPase at the base of the apparatus to support proper injectisome formation, protein secretion, and pathogen virulence. 14,15,19,22,35,39,53

The specific mechanism(s) tying ATP hydrolysis to T3SS protein secretion remain controversial and largely unclear, though bacteria expressing ATPase inactive mutants are unable to support proper protein secretion through the injectisome and are unable to initiate or sustain infection. T3SS-expressing bacteria exploit this strict link between T3SS ATPase activity and pathogen virulence by regulating ATPase function through protein interactions that appear to influence its oligomeric state and ultimately enzymatic efficiency, perhaps controlling the timing of specific infection events including micropinocytosis, lysosomal escape, and induction of macrophage apontosis. 19,222

This clear link between T3SS function and pathogen virulence has fueled several independent studies geared toward identification of small molecule inhibitors that affect T3SS function and pathogen virulence. However, determining the specific mode of action of inhibitors identified via cell-based screening methods can be exceptionally challenging and the mechanisms of action of many T3SS inhibitors remain unknown, though some have been implicated in repressing

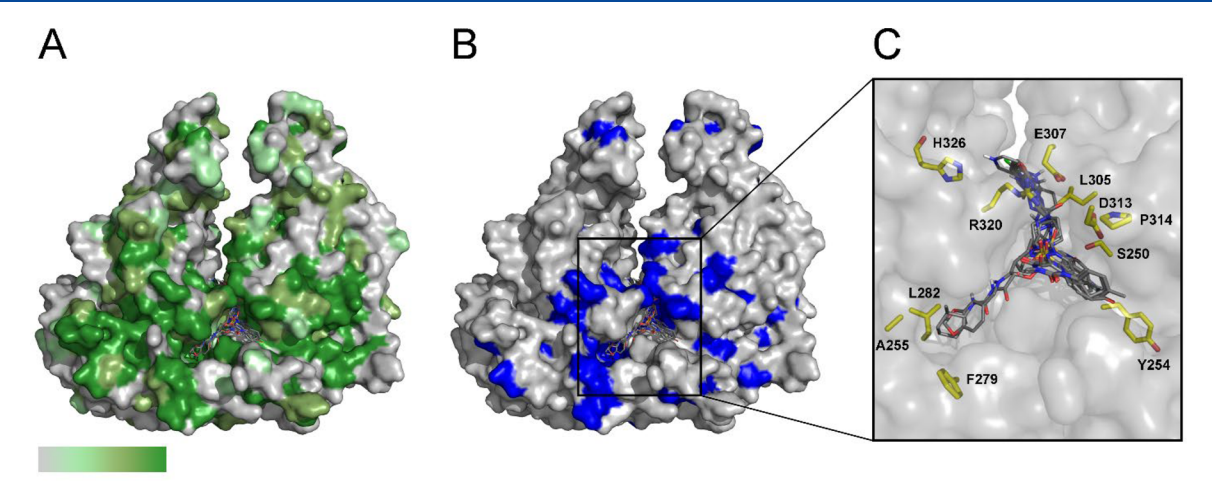


Figure 9. Sequence homology supports the potential for specific cross-pathogen T3SS ATPase inhibitors. (A) Protein sequence homology between Spa47, EscN, and FliI is displayed on the inhibitor-bound Spa47 model using a color intensity gradient to represent the degree of residue conservation (as determined using Clustal Omega). Gray coloration represents no conservation at that position and the darkest shade of green represents identical residues in each of the three aligned ATPases. Conservation between groups with strongly similar properties and those with weakly similar properties are indicated with decreasing coloration intensity, respectively. (B) Residues that are 100% conserved in Spa47, EscN, and FliI, but are not conserved in F1 ATP synthase are colored blue. (C) Side chains of select residues conserved in Spa47, EscN, and FliI, but not in F1 ATP synthase are shown as yellow sticks surrounding the ten independently docked inhibitors at the interface of Spa47 protomers.

transcription of essential T3SS genes, 56–58 preventing protein secretion through direct interaction with the external needle proteins, 59 and suppressing T3SS ATPase activity. 60,61 Recognizing the potential power of targeted inhibition studies over cell-based screens, a small number of laboratories, including our own, have specifically identified and tested T3SS ATPase inhibitors as tools for dissecting the role(s) of T3SS ATPases on T3SS function and pathogen virulence. 20,21,25,62,63

In the work presented here, we developed an in silico computational screen to test the interactions of 7.6 million drug-like compounds from the ZINC database against a protomer interface within a model of the activated Shigella Spa47 homohexameric structure. After narrowing down the list of potential inhibitors to ten, based on predicted binding strength and location, logP, and commercial availability, the putative inhibitors were tested for in vitro effect on ATP hydrolysis by recombinant Spa47 and in vivo for effect on type three secretion activity in Shigella. Seven of the ten inhibitors reduced ATPase activity by greater than 50%, and all but one of these significantly reduced effector protein secretion through the injectisome in a live cell Shigella protein secretion assay. These results demonstrate the effectiveness of the in silico screen developed here and identify a novel series of Shigella T3SS ATPase inhibitors that add to the currently small pool of T3SS ATPase inhibitors recognized to date.

While the roles of T3SS ATPase inhibitors as mechanistic tools should not go unappreciated, they have gained significant attention for their promise as nonantibiotic based therapeutics that could effectively treat infections by a broad and deadly class of human pathogens. Therapeutics designed to disarm the T3SS rather than interfering with traditional bactericidal targets such as cell wall biosynthesis and protein translation would themselves not be lethal to the bacteria, but would still prevent them from sustaining an existing infection and evading host immune responses. This would carry the benefit of minimizing impact on the patient's intestinal flora and would permit the host's immune system to clear the infection and gain immunological memory against the pathogen. The idea of

developing therapeutic T3SS ATPase inhibitors, however, has been met with concerns regarding cross-reactivity to the highly conserved active sites within essential bacterial and human ATPases such as the F and V type ATPases associated with ATP synthesis and vacuolar acidification, respectively. Bzdzion and colleagues validated this concern when they developed an *in silico* screen to identify small molecules that bound within the active site of the *E. coli* T3SS ATPase EscN, successfully identifying several competitive inhibitors against the enzyme, but finding that those strictly screened against the substrate binding site were highly toxic toward mammalian (HeLa) cells.⁶²

Looking to circumvent these cross-reactivity concerns and identify noncompetitive inhibitors, the screen we developed built upon our recent findings showing that Spa47 not only requires oligomerization to form functional active sites, but that interfering with native intermolecular interactions within the protomer interface (outside the active site) impacts active site geometry and abrogates enzyme function even when oligomerization is maintained, disarming the Shigella T3SS.³³ As described above in detail, this approach proved successful, identifying several small molecules that were effective in vitro against Spa47 activity and in vivo against Shigella T3SS function (Figure 2 and Figure 5). Extensive kinetic analysis of four of the candidates (8573, 3812, 6573, and 8771) confirmed that they are in fact noncompetitive Spa47 inhibitors with IC₅₀'s as low as 25 \pm 20 μ M (Figure 3 and Figure 7), consistent with the most efficient competitive T3SS ATPase inhibitors described to date. While moderate (micromolar) IC₅₀'s continue to impede the development and use of T3SS ATPase inhibitors as therapeutics, the targeted identification of effective noncompetitive inhibitors that exhibit low cellular toxicity marks a major milestone, as these compounds circumvent concerns about specificity, avoiding F-type ATPases critical for ATP synthesis and cell viability (Figure 4). With promising inhibitors in hand, follow-up structureactivity relationship (SAR) studies will undoubtedly shed additional light on the mechanistic details of these novel inhibitors and move them one step closer to clinical

application by exploiting their noncompetitive mode of action and T3SS ATPase-specific function while decreasing IC_{50} 's through chemical modifications that enhance solubility, affinity, and overall efficacy. Compound 8771, for example, would serve as an ideal platform for SAR studies geared toward increasing inhibitor efficiency. It already functions through a noncompetitive inhibition mechanism, reduces *Shigella* IpaC secretion *in vivo* by nearly 95%, exhibits low *Shigella* and HeLa cell cytotoxicity, and shows promise as a cross-pathogen T3SS ATPase inhibitor with robust *in vitro* ATPase inhibition across several T3SS ATPase homologues. It exhibits the highest IC_{50} of all the inhibitors examined in this study, however, essentially preventing its consideration as a therapeutic in its current form.

The appeal of noncompetitive inhibitors such as those identified in this study is their ability to effectively target T3SS ATPases while avoiding the highly conserved active site(s) of essential off-target enzymes such as F1 ATP synthase. While low cytotoxicity of the tested Spa47 inhibitors suggests that they do in fact avoid off-target ATPases, we were curious whether they remain effective against highly conserved T3SS ATPase isozymes from other organisms. Each of the ten small molecule inhibitors were tested against the *E. coli* T3SS ATPase EscN and the flagellar T3SS ATPase, FliI, from Salmonella enterica. Interestingly, the Spa47 inhibitors demonstrate remarkably similar trends in inhibition of Spa47, EscN, and FliI (Figure 8), suggesting that perhaps they exploit conservation (outside the active site) among T3SS ATPases that is not shared by off-target ATPases.

Independently aligning the Spa47 sequence to those of EscN, FliI, and both the α and β subunits of F1 ATP synthase show 40%, 37%, 27%, and 26% sequence identity, respectively; however, overall sequence conservation alone does not explain the T3SS ATPase-specific inhibition observed for these new inhibitors. Therefore, we mapped the sequence conservation of Spa47, EscN, and FliI onto the structure of Spa47 to generate a 3D conservation model (Figure 9A). The conservation model illustrates the significant degree of sequence conservation across the tested T3SS ATPases and finds that the inhibitor binding pocket in Spa47 is exceptionally well conserved. In addition, the conservation model was then modified to exclude any residues that are additionally conserved in the corresponding subunit of F1 ATP synthase (Figure 9B). This modified conservation map now specifically identifies residues that are fully conserved in Spa47, EscN, and FliI, but are not conserved in F1 ATP synthase and are presumably capable of supporting the T3SS ATPase-specific inhibition observed in this study. Examining the inhibitor binding sites within this Spa47 conservation model identifies 11 residues that line the binding pocket and are uniquely conserved within the tested T3SS ATPases while lacking conservation in F1 ATP synthase. Specifically, two distinct regions of conserved residues are uncovered, one capable of contributing to stabilizing electrostatic interactions and the other to hydrophobic effect and π stacking (Figure 9C). Furthermore, evaluation of these 11 residues in a total of seven T3SS ATPase sequences continues to demonstrate remarkable levels of conservation within the inhibitor binding site (Table S2). While intensive molecular dynamics calculations and/or high-resolution inhibitor-bound structures will certainly be required to uncover specific protein-inhibitor interactions and fuel efforts to modify inhibitor structures to optimize efficacy and solubility, these findings provide the foundation for this work and suggest that

the identified inhibitors may be broadly effective against T3SS ATPases from many important pathogens.

Taken together, the computational and experimental data presented here provide the most extensive list and in-depth characterization of noncompetitive T3SS ATPase inhibitors to date, providing insight into the role(s) of T3SS ATPases in T3SS activation and pathogen virulence and demonstrating the potential for the development of broadly effective crosspathogen T3SS ATPase inhibitors.

ASSOCIATED CONTENT

3 Supporting Information

The Supporting Information is available free of charge at https://pubs.acs.org/doi/10.1021/acs.biochem.0c00431.

Table S1 includes structures and physical characteristics of the inhibitors tested in this study, and Table S2 includes conservation information for T3SS ATPase residues within the predicted inhibitor binding sites. (PDF)

Accession Codes

UniProtKB accession numbers: Spa47, P0A1C1; F1 ATP synthase (α -subunit), P25705; F1 ATP synthase (β -subunit), P06576; EscN, Q9AJ15; FliI, P26465; InvC, B5RDL8; SsaN, P74857; YscN, P40290; and CdsN, F8KX49.

AUTHOR INFORMATION

Corresponding Author

Nicholas E. Dickenson — Department of Chemistry and Biochemistry, Utah State University, Logan, Utah 84322, United States; oorcid.org/0000-0003-1572-6077; Email: nick.dickenson@usu.edu

Authors

Heather B. Case — Department of Chemistry and Biochemistry, Utah State University, Logan, Utah 84322, United States

Dominic S. Mattock — Department of Chemistry, Truman State University, Kirksville, Missouri 63501, United States

Bill R. Miller III — Department of Chemistry, Truman State University, Kirksville, Missouri 63501, United States

Complete contact information is available at: https://pubs.acs.org/10.1021/acs.biochem.0c00431

Funding

This work was supported, in part, by a grant from the National Institute of Allergy and Infectious Disease of the National Institutes of Health under Award Number R15AI124108, and R. Gaurth Hansen endowment funds to N.E.D. The content is solely the responsibility of the authors and does not necessarily represent the official views of the National Institutes of Health. Computational resources were provided, in part, by the MERCURY supercomputer consortium under NSF Grants CHE-1229354 and CHE-1626238.

Notes

The authors declare no competing financial interest.

ACKNOWLEDGMENTS

The authors thank Saul Gonzalez for his assistance with performing Western blot analyses.

ABBREVIATIONS

AAA ATPase, ATPase associated with diverse cellular activities; AEBSF, 4-(2-aminoethyl) benzenesulfonyl fluoride hydrochloride; ATCC, American Type Culture Collection; BSA, bovine serum albumin; CBD, chitin binding domain; DTT, dithiothreitol; DMSO, dimethyl sulfoxide; GAPDH, glyceraldehyde-3-phosphate dehydrogenase; IC $_{50}$, half maximal inhibitory concentration; IPTG, Isopropyl β -D-1-thiogalactopyranoside; LPS, lipopolysaccharide; MTT, 3-(4,5-dimethylthiazol-2-yl)-2,5-diphenyltetrazolium bromide; OD600, optical density at 600 nm; PDVF, polyvinylidene fluoride; SEC, size exclusion chromatography; T3SA, type three secretion apparatus; T3SS, type three secretion system; TB, terrific broth; TSB, tryptic soy broth; TSA, tryptic soy agar.

REFERENCES

- (1) Galan, J. E., and Curtiss, R., 3rd. (1989) Cloning and molecular characterization of genes whose products allow Salmonella typhimurium to penetrate tissue culture cells. *Proc. Natl. Acad. Sci. U. S. A.* 86, 6383–6387.
- (2) Michiels, T., Wattiau, P., Brasseur, R., Ruysschaert, J. M., and Cornelis, G. (1990) Secretion of Yop proteins by Yersiniae. *Infect. Immun.* 58, 2840–2849.
- (3) Coburn, B., Sekirov, I., and Finlay, B. B. (2007) Type III secretion systems and disease. Clin. Microbiol. Rev. 20, 535-549.
- (4) Galan, J. E., Lara-Tejero, M., Marlovits, T. C., and Wagner, S. (2014) Bacterial type III secretion systems: specialized nanomachines for protein delivery into target cells. *Annu. Rev. Microbiol.* 68, 415–438.
- (5) Buttner, D. (2012) Protein export according to schedule: architecture, assembly, and regulation of type III secretion systems from plant- and animal-pathogenic bacteria. *Microbiol Mol. Biol. Rev.* 76, 262–310.
- (6) Schroeder, G. N., and Hilbi, H. (2008) Molecular pathogenesis of *Shigella* spp.: controlling host cell signaling, invasion, and death by type III secretion. *Clin. Microbiol. Rev.* 21, 134–156.
- (7) Lara-Tejero, M., and Galan, J. E. (2019) The Injectisome, a Complex Nanomachine for Protein Injection into Mammalian Cells. *EcoSal Plus 8*, ESP-0039-2018.
- (8) Chatterjee, S., Chaudhury, S., McShan, A. C., Kaur, K., and De Guzman, R. N. (2013) Structure and biophysics of type III secretion in bacteria. *Biochemistry* 52, 2508–2517.
- (9) Notti, R. Q., and Stebbins, C. E. (2016) The Structure and Function of Type III Secretion Systems. *Microbiol. Spectr.* 4, VMBF-00042015.
- (10) Enninga, J., and Rosenshine, I. (2009) Imaging the assembly, structure and activity of type III secretion systems. *Cell. Microbiol.* 11, 1462–1470.
- (11) Lunelli, M., Kamprad, A., Burger, J., Mielke, T., Spahn, C. M. T., and Kolbe, M. (2020) Cryo-EM structure of the Shigella type III needle complex. *PLoS Pathog.* 16, No. e1008263.
- (12) Hu, B., Morado, D. R., Margolin, W., Rohde, J. R., Arizmendi, O., Picking, W. L., Picking, W. D., and Liu, J. (2015) Visualization of the type III secretion sorting platform of Shigella flexneri. *Proc. Natl. Acad. Sci. U. S. A.* 112, 1047–1052.
- (13) Adam, P. R., Dickenson, N. E., Greenwood, J. C., Picking, W. L., and Picking, W. D., 2nd (2014) Influence of oligomerization state on the structural properties of invasion plasmid antigen B from Shigella flexneri in the presence and absence of phospholipid membranes. *Proteins: Struct., Funct., Genet.* 82, 3013–3022.
- (14) Akeda, Y., and Galan, J. E. (2004) Genetic analysis of the Salmonella enterica type III secretion-associated ATPase InvC defines discrete functional domains. *J. Bacteriol.* 186, 2402–2412.
- (15) Jouihri, N., Sory, M. P., Page, A. L., Gounon, P., Parsot, C., and Allaoui, A. (2003) MxiK and MxiN interact with the Spa47 ATPase and are required for transit of the needle components MxiH and MxiI,

- but not of Ipa proteins, through the type III secretion apparatus of Shigella flexneri. *Mol. Microbiol.* 49, 755–767.
- (16) Woestyn, S., Allaoui, A., Wattiau, P., and Cornelis, G. R. (1994) YscN, the putative energizer of the Yersinia Yop secretion machinery. *J. Bacteriol.* 176, 1561–1569.
- (17) Zarivach, R., Vuckovic, M., Deng, W., Finlay, B. B., and Strynadka, N. C. (2007) Structural analysis of a prototypical ATPase from the type III secretion system. *Nat. Struct. Mol. Biol.* 14, 131–137.
- (18) Akeda, Y., and Galan, J. E. (2005) Chaperone release and unfolding of substrates in type III secretion. *Nature* 437, 911–915.
- (19) Case, H. B., and Dickenson, N. E. (2018) MxiN Differentially Regulates Monomeric and Oligomeric Species of the Shigella Type Three Secretion System ATPase Spa47. *Biochemistry* 57, 2266–2277.
- (20) Case, H. B., Mattock, D. S., and Dickenson, N. E. (2018) Shutting Down Shigella Secretion: Characterizing Small Molecule Type Three Secretion System ATPase Inhibitors. *Biochemistry* 57, 6906–6916.
- (21) Swietnicki, W., Carmany, D., Retford, M., Guelta, M., Dorsey, R., Bozue, J., Lee, M. S., and Olson, M. A. (2011) Identification of small-molecule inhibitors of Yersinia pestis Type III secretion system YscN ATPase. *PLoS One 6*, No. e19716.
- (22) Minamino, T., and MacNab, R. M. (2000) FliH, a soluble component of the type III flagellar export apparatus of Salmonella, forms a complex with FliI and inhibits its ATPase activity. *Mol. Microbiol.* 37, 1494–1503.
- (23) Blaylock, B., Riordan, K. E., Missiakas, D. M., and Schneewind, O. (2006) Characterization of the Yersinia enterocolitica type III secretion ATPase YscN and its regulator, YscL. *J. Bacteriol.* 188, 3525–3534.
- (24) Stone, C. B., Bulir, D. C., Emdin, C. A., Pirie, R. M., Porfilio, E. A., Slootstra, J. W., and Mahony, J. B. (2011) Chlamydia Pneumoniae CdsL Regulates CdsN ATPase Activity, and Disruption with a Peptide Mimetic Prevents Bacterial Invasion. *Front Microbiol.* 2, 21.
- (25) Gong, L., Lai, S. C., Treerat, P., Prescott, M., Adler, B., Boyce, J. D., and Devenish, R. J. (2015) Burkholderia pseudomallei type III secretion system cluster 3 ATPase BsaS, a chemotherapeutic target for small-molecule ATPase inhibitors. *Infect. Immun.* 83, 1276–1285.
- (26) Formal, S. B., Dammin, G. J., Labrec, E. H., and Schneider, H. (1958) Experimental Shigella infections: characteristics of a fatal infection produced in guinea pigs. *J. Bacteriol.* 75, 604–610.
- (27) Burgess, J. L., Burgess, R. A., Morales, Y., Bouvang, J. M., Johnson, S. J., and Dickenson, N. E. (2016) Structural and Biochemical Characterization of Spa47 Provides Mechanistic Insight into Type III Secretion System ATPase Activation and Shigella Virulence Regulation. *J. Biol. Chem.* 291, 25837–25852.
- (28) Abrahams, J. P., Leslie, A. G., Lutter, R., and Walker, J. E. (1994) Structure at 2.8 A resolution of F1-ATPase from bovine heart mitochondria. *Nature* 370, 621–628.
- (29) PyMOL Molecular Graphics System, version 1.8, Schrödinger, LLC.
- (30) Dassault Systèmes BIOVIA Discover Studio ViewerPro, Version 5.0, Dassault Systèmes, San Diego, 2003.
- (31) Sterling, T., and Irwin, J. J. (2015) ZINC 15-Ligand Discovery for Everyone. J. Chem. Inf. Model. 55, 2324-2337.
- (32) O'Boyle, N. M., Banck, M., James, C. A., Morley, C., Vandermeersch, T., and Hutchison, G. R. (2011) Open Babel: An open chemical toolbox. *J. Cheminform* 3, 33.
- (33) Demler, H. J., Case, H. B., Morales, Y., Bernard, A. R., Johnson, S. J., and Dickenson, N. E. (2019) Interfacial amino acids support Spa47 oligomerization and Shigella type three secretion system activation. *Proteins: Struct., Funct., Genet.* 87, 931–942.
- (34) Alhossary, A., Handoko, S. D., Mu, Y., and Kwoh, C. K. (2015) Fast, accurate, and reliable molecular docking with QuickVina 2. *Bioinformatics* 31, 2214–2216.
- (35) Burgess, J. L., Jones, H. B., Kumar, P., Toth, R. T., Middaugh, C. R., Antony, E., and Dickenson, N. E. (2016) Spa47 is an oligomerization-activated type three secretion system (T3SS) ATPase from Shigella flexneri. *Protein Science: A Publication of the Protein Society* 25, 1037–1048.

- (36) Parsot, C., Ménard, R., Gounon, P., and Sansonetti, P. J. (1995) Enhanced secretion through the Shigella flexneri Mxi-Spa translocon leads to assembly of extracellular proteins into macromolecular structures. *Mol. Microbiol.* 16, 291–300.
- (37) Bernard, A. R., Jessop, T. C., Kumar, P., and Dickenson, N. E. (2017) Deoxycholate-Enhanced Shigella Virulence Is Regulated by a Rare π-Helix in the Type Three Secretion System Tip Protein IpaD. *Biochemistry* 56, 6503–6514.
- (38) Burgess, J. L., Case, H. B., Burgess, R. A., and Dickenson, N. E. (2020) Dominant negative effects by inactive Spa47 mutants inhibit T3SS function and Shigella virulence. *PLoS One* 15, No. e0228227.
- (39) Kentner, D., Martano, G., Callon, M., Chiquet, P., Brodmann, M., Burton, O., Wahlander, A., Nanni, P., Delmotte, N., Grossmann, J., Limenitakis, J., Schlapbach, R., Kiefer, P., Vorholt, J. A., Hiller, S., and Bumann, D. (2014) Shigella reroutes host cell central metabolism to obtain high-flux nutrient supply for vigorous intracellular growth. *Proc. Natl. Acad. Sci. U. S. A. 111*, 9929–9934.
- (40) Deng, W., Marshall, N. C., Rowland, J. L., McCoy, J. M., Worrall, L. J., Santos, A. S., Strynadka, N. C. J., and Finlay, B. B. (2017) Assembly, structure, function and regulation of type III secretion systems. *Nat. Rev. Microbiol.* 15, 323–337.
- (41) Schroeder, G. N., Jann, N. J., and Hilbi, H. (2007) Intracellular type III secretion by cytoplasmic Shigella flexneri promotes caspase-1-dependent macrophage cell death. *Microbiology* 153, 2862–2876.
- (42) Carayol, N., and Tran Van Nhieu, G. (2013) The inside story of Shigella invasion of intestinal epithelial cells. *Cold Spring Harbor Perspect. Med.* 3, a016717.
- (43) Phalipon, A., and Sansonetti, P. J. (2007) Shigella's ways of manipulating the host intestinal innate and adaptive immune system: a tool box for survival? *Immunol. Cell Biol.* 85, 119–129.
- (44) Tobe, T., Yoshikawa, M., Mizuno, T., and Sasakawa, C. (1993) Transcriptional control of the invasion regulatory gene virB of Shigella flexneri: activation by virF and repression by H-NS. *J. Bacteriol.* 175, 6142–6149.
- (45) Tobe, T., Nagai, S., Okada, N., Adler, B., Yoshikawa, M., and Sasakawa, C. (1991) Temperature-regulated expression of invasion genes in Shigella flexneri is controlled through the transcriptional activation of the virB gene on the large plasmid. *Mol. Microbiol. 5*, 887–893.
- (46) Mizusaki, H., Takaya, A., Yamamoto, T., and Aizawa, S. (2008) Signal pathway in salt-activated expression of the Salmonella pathogenicity island 1 type III secretion system in Salmonella enterica serovar Typhimurium. *J. Bacteriol.* 190, 4624–4631.
- (47) Stensrud, K. F., Adam, P. R., La Mar, C. D., Olive, A. J., Lushington, G. H., Sudharsan, R., Shelton, N. L., Givens, R. S., Picking, W. L., and Picking, W. D. (2008) Deoxycholate interacts with IpaD of Shigella flexneri in inducing the recruitment of IpaB to the type III secretion apparatus needle tip. *J. Biol. Chem.* 283, 18646—18654.
- (48) Dickenson, N. E., and Picking, W. D. (2012) Forster resonance energy transfer (FRET) as a tool for dissecting the molecular mechanisms for maturation of the Shigella type III secretion needle tip complex. *Int. J. Mol. Sci.* 13, 15137–15161.
- (49) Barta, M. L., Guragain, M., Adam, P., Dickenson, N. E., Patil, M., Geisbrecht, B. V., Picking, W. L., and Picking, W. D. (2012) Identification of the bile salt binding site on IpaD from Shigella flexneri and the influence of ligand binding on IpaD structure. *Proteins: Struct., Funct., Genet.* 80, 935–945.
- (50) Straley, S. C., Plano, G. V., Skrzypek, E., Haddix, P. L., and Fields, K. A. (1993) Regulation by Ca2+ in the Yersinia low-Ca2+ response. *Mol. Microbiol.* 8, 1005–1010.
- (51) Epler, C. R., Dickenson, N. E., Olive, A. J., Picking, W. L., and Picking, W. D. (2009) Liposomes recruit IpaC to the Shigella flexneri type III secretion apparatus needle as a final step in secretion induction. *Infect. Immun.* 77, 2754–2761.
- (52) Adam, P. R., Patil, M. K., Dickenson, N. E., Choudhari, S., Barta, M., Geisbrecht, B. V., Picking, W. L., and Picking, W. D. (2012) Binding affects the tertiary and quaternary structures of the Shigella

- translocator protein IpaB and its chaperone IpgC. Biochemistry 51, 4062-4071.
- (53) Majewski, D. D., Worrall, L. J., Hong, C., Atkinson, C. E., Vuckovic, M., Watanabe, N., Yu, Z., and Strynadka, N. C. J. (2019) Cryo-EM structure of the homohexameric T3SS ATPase-central stalk complex reveals rotary ATPase-like asymmetry. *Nat. Commun.* 10, 626
- (54) Gu, L., Zhou, S., Zhu, L., Liang, C., and Chen, X. (2015) Small-Molecule Inhibitors of the Type III Secretion System. *Molecules 20*, 17659–17674.
- (55) Fasciano, A. C., Shaban, L., and Mecsas, J. (2019) Promises and Challenges of the Type Three Secretion System Injectisome as an Antivirulence Target. *EcoSal Plus 8*, ESP-0032-2018. DOI: 10.1128/ecosalplus.ESP-0032-2018.
- (56) Gauthier, A., Robertson, M. L., Lowden, M., Ibarra, J. A., Puente, J. L., and Finlay, B. B. (2005) Transcriptional inhibitor of virulence factors in enteropathogenic Escherichia coli. *Antimicrob. Agents Chemother.* 49, 4101–4109.
- (57) Zhang, Y., Liu, Y., Wang, T., Deng, X., and Chu, X. (2018) Natural compound sanguinarine chloride targets the type III secretion system of Salmonella enterica Serovar Typhimurium. *Biochem Biophys Rep* 14, 149–154.
- (58) Li, J., Lv, C., Sun, W., Li, Z., Han, X., Li, Y., and Shen, Y. (2013) Cytosporone B, an inhibitor of the type III secretion system of Salmonella enterica serovar Typhimurium. *Antimicrob. Agents Chemother.* 57, 2191–2198.
- (59) Bowlin, N. O., Williams, J. D., Knoten, C. A., Torhan, M. C., Tashjian, T. F., Li, B., Aiello, D., Mecsas, J., Hauser, A. R., Peet, N. P., Bowlin, T. L., and Moir, D. T. (2014) Mutations in the Pseudomonas aeruginosa needle protein gene pscF confer resistance to phenoxyacetamide inhibitors of the type III secretion system. *Antimicrob. Agents Chemother.* 58, 2211–2220.
- (60) Anantharajah, A., Buyck, J. M., Sundin, C., Tulkens, P. M., Mingeot-Leclercq, M. P., and Van Bambeke, F. (2017) Salicylidene Acylhydrazides and Hydroxyquinolines Act as Inhibitors of Type Three Secretion Systems in Pseudomonas aeruginosa by Distinct Mechanisms. *Antimicrob. Agents Chemother.* 61, e02566–02516.
- (61) Anantharajah, A., Faure, E., Buyck, J. M., Sundin, C., Lindmark, T., Mecsas, J., Yahr, T. L., Tulkens, P. M., Mingeot-Leclercq, M. P., Guery, B., and Van Bambeke, F. (2016) Inhibition of the Injectisome and Flagellar Type III Secretion Systems by INP1855 Impairs Pseudomonas aeruginosa Pathogenicity and Inflammasome Activation. *J. Infect. Dis.* 214, 1105–1116.
- (62) Bzdzion, L., Krezel, H., Wrzeszcz, K., Grzegorek, I., Nowinska, K., Chodaczek, G., and Swietnicki, W. (2017) Design of small molecule inhibitors of type III secretion system ATPase EscN from enteropathogenic Escherichia coli. *Acta Biochim. Pol.* 64, 49–63.
- (63) Grishin, A. V., Luyksaar, S. I., Kapotina, L. N., Kirsanov, D. D., Zayakin, E. S., Karyagina, A. S., and Zigangirova, N. A. (2018) Identification of chlamydial T3SS inhibitors through virtual screening against T3SS ATPase. *Chem. Biol. Drug Des.* 91, 717–727.